# Tomas Bata University in Zlín

Doctoral Thesis Summary

# Hybrid nanomaterials for photoanodes in photoelectrochemical water splitting

## Hybridní nanomateriály pro fotoanody k fotoelektrochemickému štěpení vody

Author:               Ali Can Güler, M.Sc., Ph.D.

Degree programme:     P3972 Nanotechnology and advanced materials

Degree course:        3942V006 Nanotechnology and Advanced Materials

Supervisor:           Prof. Ing. et Ing. Ivo Kuřitka, Ph.D. et Ph.D.

External Examiners:   prof. Mgr. Aleš Mráček, Ph.D.

                      Ing. Vojtech Nádaždy, CSc.

Zlín, February 2024

# DEDICATION

This PhD thesis is dedicated to my parents (Duriye GÜLER and Salih GÜLER).

# Contents

# ABSTRACT

The urgent need for clean and renewable energy sources has prompted intense research in the field of solar-driven water splitting, with a specific focus on photoanode materials. In this context, this doctoral dissertation investigated the development of photoanode materials to advance the efficiency of photoelectrochemical water splitting, emphasizing the paramount importance of modifying charge dynamics and enhancing light harvesting capacity. Multifunctional ZnO in various nanoforms was chosen as the primary light absorber in the multi-component nanocomposite systems that were actualized by three well-established strategies.

These strategies include surface modification, simultaneous effects of conductive metal coating and gradient impurity element doping, and photosensitization by a narrow band gap semiconductor. The adopted methodologies provided a visible light activity to ZnO-based photoanodes and unveiled several vital factors influencing photoelectrochemical performance. Employing cutting-edge spectroscopic and microscopic techniques, morphological, crystallographic, optical, and electrical properties and their significance on photoelectrochemical water splitting were comprehensively analyzed.

The outcomes of this research deepen our understanding of photoanode materials and offer practical insights for developing highly efficient and stable photoelectrodes. This dissertation will hopefully serve as a valuable contribution to the field, addressing the challenges associated with harnessing solar energy for clean and renewable energy production.


Key words: *Photoelectrochemical, heterojunction photoanode, ZnO nanodendrites, BiVO$_4$, electrodeposition.*

# ABSTRAKT

Naléhavá potřeba čistých a obnovitelných zdrojů energie podnítila intenzivní výzkum v oblasti solárního štěpení vody se specifickým zaměřením na fotoanodové materiály. V této souvislosti se tato disertační práce zabývala vývojem fotoanodových materiálů pro zvýšení účinnosti fotoelektrochemického štěpení vody, zdůrazňujíc prvořadý význam modifikace dynamiky náboje a zvýšení kapacity sběru světla. Multifunkční ZnO v různých nanoformách byl zvolen jako primární absorbér světla ve vícesložkových nanokompozitních systémech, které byly vylepšeny pomocí tří již dobře zavedených strategií.

Tyto strategie zahrnují povrchovou úpravu, souběžné účinky vodivého kovového povlaku a gradientního dopování příměsovým prvkem a fotosenzibilizaci polovodičem s úzkým zakázaným pásem. Adaptované metodiky umožnily dosáhnout u fotoanod na bázi ZnO nejen aktivitu ve viditelném světle, ale také odhalily několik klíčových faktorů ovlivňujících fotoelektrochemický výkon. S využitím nejmodernějších spektroskopických a mikroskopických technik byly komplexně analyzovány morfologické, krystalografické, optické a elektrické vlastnosti a jejich význam pro fotoelektrochemické štěpení vody.

Výsledky tohoto výzkumu nejen prohlubují naše znalosti o fotoanodových materiálech, ale nabízejí také praktické poznatky pro vývoj vysoce účinných a stabilních fotoelektrod. Doufejme, že tato dizertační práce poslouží jako cenný příspěvek v oboru a bude řešit problémy spojené s využíváním solární energie pro výrobu čisté a obnovitelné energie.

Klíčová slova: *Fotoelektrochemické, heteropřechodová fotoanoda, nanodendrity oxidu zinečnatého, vanadičnan bismutitý, elektrodepozice.*

# ACKNOWLEDGEMENTS

I wish to extend my heartfelt gratitude to my esteemed advisor, Prof. Ivo Kuřitka, whose expertise and knowledge enlightened me during my PhD studies, for his invaluable mentorship throughout this research.

I extend my profound appreciation to all my colleagues who provided exceptional assistance and guidance in laboratory operations conducted as part of this research.

I would like to express my gratitude to Assoc. Prof. José Joaquín Velázquez García from the FunGlass Centre at the Alexander Dubček University in Trenčín and Prof. Dr. Radim Beránek from the Institute of Electrochemistry at Ulm University for their valuable guidance and allowing me to use their laboratory facilities during my internships.

Additionally, I am incredibly grateful to my precious mother, Duriye GÜLER, my father, Salih GÜLER and my sister, Özlem GÜLER, who have supported me in every aspect throughout my life.

# 1. INTRODUCTION

The escalating demands for energy driven by population growth and industrial expansion surpass the finite resources available on a global scale. Most of the global energy demands are supplied through the utilization of fossil fuels owing to their high energy density. Various estimations indicate that fossil fuel depletion will likely occur within the coming decades [1,2]. The overconsumption of fossil fuels contributes to global warming by releasing large quantities of greenhouse gases such as carbon dioxide. For instance, coal-fired power plants in China are responsible for 40% of total carbon emissions, resulting in a rise in global temperatures [3].

The utilization of renewable energy offers numerous potential advantages, such as mitigating greenhouse gas emissions, diversifying energy sources, and decreasing reliance on fossil fuel consumption. According to the International Renewable Energy Agency, it is anticipated that renewable sources have the potential to account for 90% of the world's energy supply by 2050 [4]. Serious measures are being taken globally to reduce greenhouse gas emissions as well as increasing the amount of energy coming from renewable sources. In this respect, the European Union has pledged to decrease its net greenhouse gas emissions by at least 55% by 2030 under the European Climate Law [5]. Of particular note, the Czech Republic's climate and energy plan predicts that the share of renewable energy in gross final consumption will reach 30% with the installation of 10 GWe solar and 1.5 GWe wind by 2030, five times the current capacity [6].

Energy can be stored in the bonds formed by chemical compounds and regained through exothermic reactions [7]. Chemical energy storage is one of the four possible methods and has serious advantages over the other three methods (mechanical, thermal, and electrical) [8,9]. Hydrogen is readily produced through water splitting. Several ways to achieve this include thermolysis, thermochemical water splitting, photobiological water cleavage, and electrochemical and photoelectrochemical (PEC) water splitting [10]. For being ecologically friendly and efficient, among all the methods, the PEC process is the most feasible to separate water. Nevertheless, to compete with non-renewable energy sources, a lot of effort and investment still needs to be devoted to developing more efficient and affordable electrode materials.

# 2. THEORETICAL BACKGROUND

## 2.1 Photoelectrochemical water splitting

PEC water splitting has been intensively investigated as an artificial photosynthesis technology to disassociate water into hydrogen and oxygen since the pioneering demonstration by Honda and Fujishima [11,12]. This process involves using a thin semiconductor film that generates charge carriers when exposed to light with appropriate energy. The photogenerated electron-hole pairs facilitate the redox reactions at the electrode-electrolyte interface. From a thermodynamic point of view, the water-splitting reaction requires 285.8 kJ/mol of energy input under standard conditions of room temperature and pressure [13]. This is equivalent to the energy released during the combustion of hydrogen to form water. The energy is produced by the Gibbs free energy (237.2 kJ/mol) and the heat released by the reaction (48.6 kJ/mol) [14]. Combustion is a chemical reaction in which $H_2$ as a fuel and $O_2$ as an oxidant react in an exothermic reaction, and water is formed (equation (2.1)). In the reverse reaction (equation (2.2)), a certain amount of energy corresponding to the Gibbs energy must be provided to split water into hydrogen and oxygen.

$$H_2(g) + \frac{1}{2}O_2(g) \rightarrow H_2O(l) + 237.2 \text{ kJ/mol} + 48.6 \text{ kJ/mol} \qquad (2.1)$$

$$H_2O(l) + 237.2 \text{ kJ/mol} + 48.6 \text{ kJ/mol} \rightarrow H_2(g) + \frac{1}{2}O_2(g) \qquad (2.2)$$
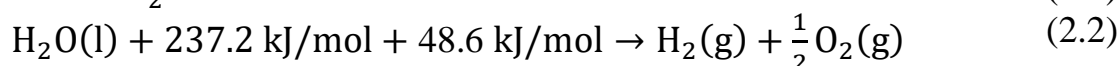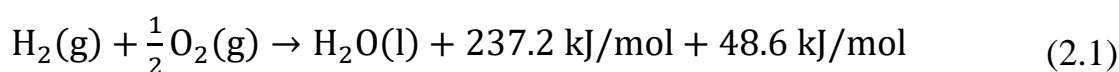
The whole PEC water splitting process involves two half-cell reactions that are oxygen evolution reaction (OER), which occurs via four electrons in a photoanode and hydrogen evolution reaction (HER), which occurs via a two-electron process in a photocathode [15]. The two half-cell reactions and the overall PEC reaction are depicted in the following equations (2.3), (2.4), and (2.5), respectively:

$$\text{OER} \quad : 2H_2O(l) \rightarrow O_2(g) + 4H^+ + 4e^- \quad E^0_{ox} = 1.23 \text{ V vs NHE} \qquad (2.3)$$

$$\text{HER} \quad : 4H^+ + 4e^- \rightarrow 2H_2 \qquad\qquad E^0_{red} = 0 \text{ V vs NHE} \qquad (2.4)$$

$$\text{Overall: } 2H_2O(l) \rightarrow 2O_2(g) + 2H_2(g) \qquad (2.5)$$
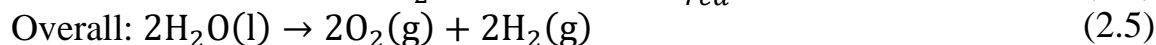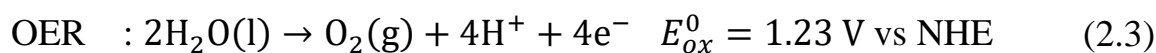
Here, $E^0_{ox}$ and $E^0_{red}$ are standard water oxidation potential and water reduction potential, respectively. These quantities are given with respect to normal hydrogen electrode (NHE) at pH 0 [16]. When equations (2.3) and (2.4) are compared, it is seen that four holes are required to produce one mole of oxygen,

whereas only two electrons are involved in the reaction to generate one mole of hydrogen so that OER with a much higher energy barrier is thermodynamically and kinetically more demanding than HER. Therefore, the OER is regarded as the primary limiting step of PEC water splitting.

### 2.1.1 Working principle of PEC water splitting

There are three types of PEC water splitting configurations: 1) n-type semiconductor as photoanode and HER at the counter electrode (such as Pt); 2) p-type semiconductor as a photocathode and OER at the counter electrode; and 3) n-type and p-type semiconductors as photoanode and photocathode for simultaneously OER and HER, respectively. In general, and within the scope of this thesis, the n-type semiconductor photoanode-based PEC cell is preferred. Accordingly, this type of PEC configuration consists of four steps: 1) light absorption by photoanode and generation of photogenerated charge carriers; 2) charge separation inside photoanode and at electrode-electrolyte interface; 3) charge transportation within photoanode; and 4) process of the surface reaction of water reduction and oxidation.

Under solar irradiation, the electron in the photoanode is stimulated from the valence band (VB) to the unoccupied conduction band (CB). This occurs when the electron absorbs photons with energy equal to or greater than the bandgap, leaving behind a hole in the valence band. Then, most electrons transfer to the cathode through the external circuit and drive HER, while most holes are injected into the surface of the photoanode and drive OER.

### 2.1.2 Photoanodes

Photoanodes are crucial constituents in a PEC water oxidation system. They are amenable to harvesting solar energy and generating charge carriers to produce oxygen through OER. As mentioned before, the photoanode material for OER should be chosen among n-type semiconductors. The band bending at the interface between electrode and electrolyte induces an electric field, which subsequently accelerates holes towards the material's surface [17]. Different from this, the band gap of the semiconductor is a vital characteristic because it determines the extent to which solar irradiance can be absorbed. A suitable band gap is expected to be in the range of 2.0-3.2 eV [18]. Equally important consideration should be given to the band edge positions. For an ideal water-

splitting semiconductor, the VB must be above the hydrogen evolution potential at 0 V to work as a photocathode, while the CB must be below the oxygen evolution potential at 1.23 V to work as a photoanode (on the electrochemical scale relative to normal hydrogen electrode) [19]. These are the main considerations for selecting a photoanode to enhance the water-splitting efficiency.

## 2.2 Zinc Oxide

### 2.2.1 Material characteristics of ZnO

ZnO is a group II-VI semiconductor metal oxide with a direct band gap of approximately 3.2 eV and a large exciton binding energy of 60 meV at room temperature [20]. The most thermodynamically stable form of ZnO under environmental conditions is the hexagonal wurtzite structure [21]. In this crystal structure, two interpenetrating hexagonal close-packed (hcp) sublattices comprise four atoms per a unit cell of one type. These hcp sublattices are displaced with respect to each other along the c-axis. In a tetrahedral, every atom of one kind (Zn) is surrounded by four atoms of another kind (O) or vice versa [22]. Hexagonal ZnO crystal has a polar basal $O^{-2}$ plane $(00\bar{1})$ and top positive $Zn^{+2}$ plane (001), and non-polar $(\bar{1}00)$, $(\bar{1}10)$ and $(0\bar{1}0)$ lateral facets [23], as indicated in **Fig. 2.1**. The primary growth direction of ZnO crystal is in the (001) direction due to the larger surface energy of the polar plane compared to the non-polar plane [24].
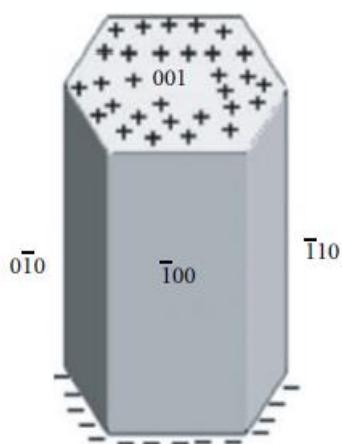


*Fig. 2.1: Hexagonal prism showing different crystal facets. Adapted from reference [24].*

### 2.2.2  Application of ZnO in PEC water splitting

Over the past few decades, numerous metal oxide semiconductors have been used as photoanodes in water splitting due to their exceptional chemical stability, affordability, tuneable band gaps, and appropriate band edge positions [25]. ZnO with n-type conductivity is an auspicious material for harnessing solar energy material because of its light-harvesting capability due to fine morphology, high electron mobility assuring rapid carrier transport, many surface trap sites improving charge carrier separation, and suitable band structure can provide holes with strong oxidation ability [26]. Furthermore, ZnO's CB and VB edge positions lie at - 0.31 V vs NHE and 2.89 V vs NHE, respectively, and are suitable for water oxidation reactions [27]. Even though all the characteristics listed above contribute a lot to the photoanode performance of ZnO in PEC water splitting, its wide band gap is referred to as the main challenge to obtain optimal photoconversion efficiency since a small portion of the total solar radiation, approximately 4%, remains to power the water splitting process. New material designs are therefore highly required to achieve maximum performance from ZnO as a photoanode in PEC water splitting.

## 2.3  Strategies for improving PEC performance of ZnO

### 2.3.1  The morphology control of ZnO

ZnO has a variety of nanostructures whose configurations are more diverse than any existing nanomaterial, such as carbon nanotubes [28]. At present, these morphologies, including nanoparticles (NPs), nanorods (NRs), nanosheets, nanotetrapods, as well as nanodendrites can be facilely fabricated by various physical and chemical synthesis methods [29,30]. Among almost all nanostructures, one-dimensional (1D) nanostructures like NRs provide several advantages in terms of charge dynamics. When the radial dimension of the NRs is equal to or smaller than the characteristic length of some essential solid-state phenomena such as the exciton Bohr radius, exciton diffusion length, wavelength of the light, phonon mean free path, etc., the physical properties of the semiconductor can be modified on the confined surfaces of the nanorods [31].

More scientific efforts have been dedicated to fabricating three-dimensional (3D) hierarchical nanostructures from low-dimensional subunits. In comparison with 1D morphologies, 3D complex ZnO morphologies have a larger active

13

surface area, resulting in a rapid charge transfer process and water oxidation kinetics. The low-dimensional subunits, such as tiny branches grown on the primarily grown nanorods scaffolds, provide a short diffusion path of photogenerated charge carriers, fast charge extraction efficiency, and a large area, leading to an excellent performance in photocatalytic and photoelectrochemical reactions [32].

The objective of controlling the morphology of ZnO nanomaterials is to increase the interfacial area between the semiconductor photoanode and electrolyte or to modify the surface roughness of the electrode. This allows for greater exposure of reaction sites and reduces the distance over which carriers transport, but control of morphology is needed to combine with other methods to improve the light-harvesting ability of ZnO.

### 2.3.2  Heterostructure fabrication of ZnO

The fabrication of heterostructure with appropriate band alignment appears to be a very effective approach to enhance the activity of photoanode in PEC water splitting. Among various methods such as quantum dot sensitization [33], p-n junction [34], Z scheme system [35], passivation layer [36], and co-catalyst for OER [37], in the context of this thesis, the heterostructures of ZnO have been mainly fabricated using type-II heterojunction and the surface plasmon resonance of noble metals sensitization. These are described in the following section below.

### 2.3.3  Fabrication of the ZnO based on type II heterojunction

In a type-II heterojunction, as shown in **Fig. 2.2**, the electrons generated by light in semiconductor B flow into semiconductor A, while the holes generated in semiconductor A migrate to semiconductor B. This process creates spatial separation between the photogenerated electron-hole pairs [38]. Besides, the efficient charge separation in type-II heterojunction provides improved charge carrier dynamics. A narrow bandgap semiconductor (B) is generally combined with a wide bandgap semiconductor (A) to form a heterojunction and extend the absorption of sun light [39].
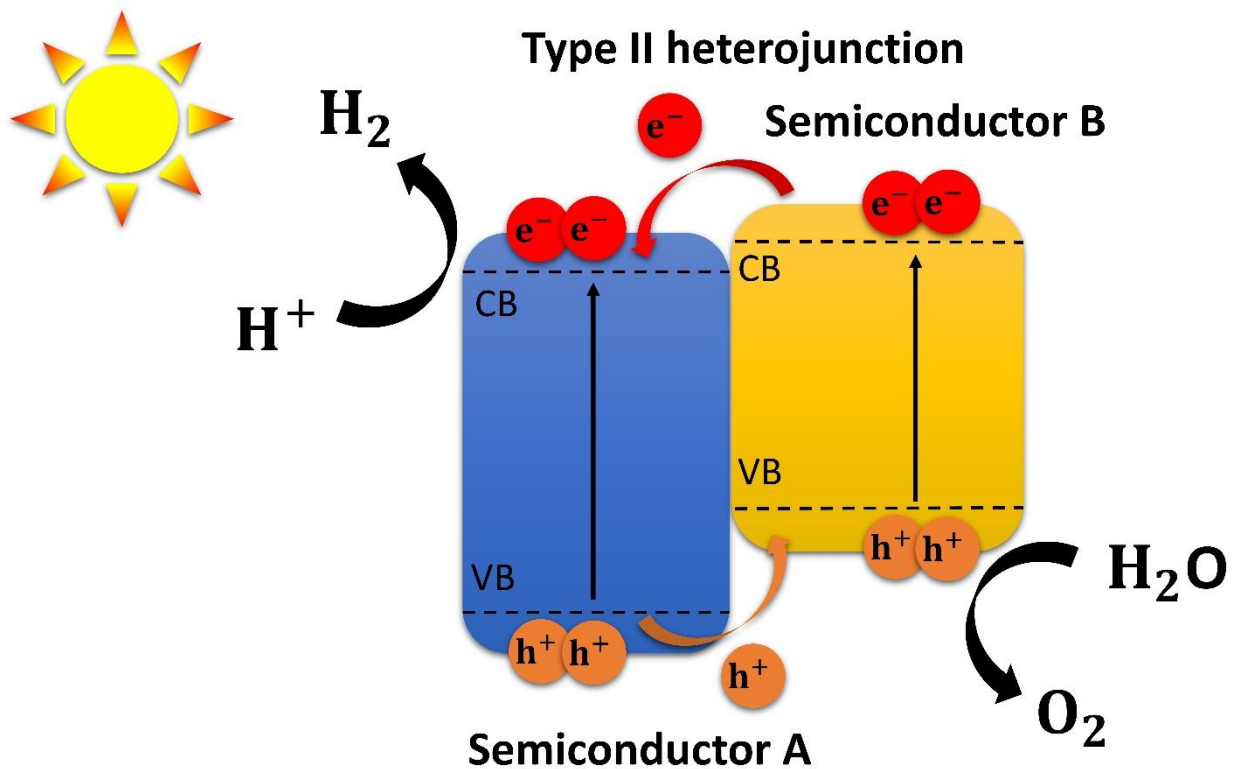
*Fig. 2.2: Illustration of the band alignment type-II heterojunction.*

### 2.3.4 The fabrication of heterostructure of ZnO based on the surface plasmon resonance of noble metal and gradient doping

Sensitization of semiconductor photoanode with plasmonic NPs can overcome the main PEC limitations, such as charge carrier diffusion and low light absorption [40]. The surface plasmon resonance (SPR) phenomenon occurs when the electron oscillation frequency on the surface of some noble metals (Au, Ag, Pt or Cu) has the same frequency as the incident electromagnetic radiation. At this point, the metal NPs have the ability to absorb visible light [41]. **Fig. 2.3** displays that the SPR-induced photogenerated carriers in the metal NPs can be effectively transferred to the CB of the semiconductor, leading to the visible light activity of the heterostructure system. This efficient charge transfer results in electron-deficiency in metal and electron richness in semiconductors, notably enhancing the overall PEC efficiency [42].
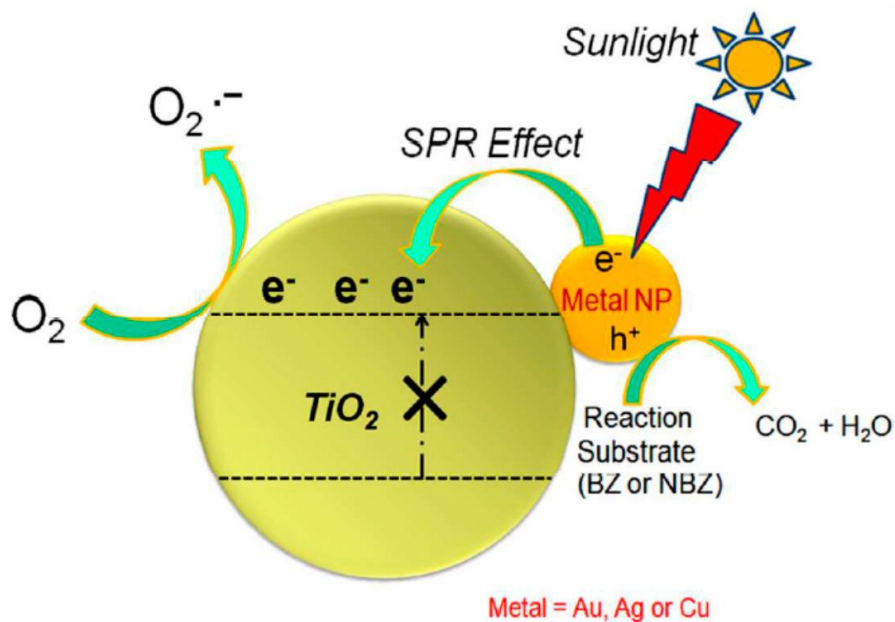
*Fig. 2.3: Surface plasmon resonance (SPR) effect of metal nanoparticles on a semiconductor under sunlight irradiation. Adapted from reference* [42].

Another beneficial approach to accomplish good carrier separation in a semiconductor photoanode is the band bending (built-in electric field) formation at the metal-semiconductor interface [43]. In the PEC water splitting field, a gradient dopant profile was recently reported as a new route to facilitate the carrier separation through the dispersion of band bending in a broader zone in the nanomaterial system, so many more electrons can accumulate on the surface and escape to vacuum level [44].

## 2.4  Design considerations for the novel photoanode materials

The following sections will discuss the physical and chemical properties of the chosen functionalization materials and their previous literature studies to emphasize why these design considerations were implemented.

The first study deals with the impact of morphological evolution on the PEC properties of ZnO NRs. Polyethyleneimine (PEI), a cationic polymer with vast amount of side amino groups, was utilized as a cation surfactant in the growth solution [45]. PEI protonates in a wide range of pH (3-11) and thus tends to be positively charged and attracted to the negatively charged non-polar surfaces of ZnO NRs [46]. In this way, PEI inhibits the radial crystal growth and produces a large surface area. Recently, Sun et al. reported the synergistic influence of PEI

and ammonia on the nanoarchitecture of ZnO nanoforests for PEC water splitting [47]. Here, the ZnO nanoforests stood out with a maximum current density of 0.919 mA.cm$^{-2}$ at 1.2 V (vs Ag/AgCl) as the charge migration improved.

The second study discusses the synergistic effect of co-occurring gradient doping and surface plasmon modification of Au-decorated ZnO NRs. Gold (Au) is the most prominent material among plasmonic nanoparticles, exhibiting strong optical absorbance and scattering properties in the visible region. Electromagnetic radiation with a much larger wavelength than the size of Au NPs can generate collective oscillations of the free electrons in metal across the NPs [40]. The SPR band of Au NPs typically lies between 517 and 575 nm [48]. The SPR phenomenon associated with plasmonic NPs helps in the suppression of charge recombination by acting as electron trapping centres, thereby promoting the efficiency of PEC cells [49]. In a study, Au surface plasmon capping generated a six-fold enhancement in the near band gap emission of ZnO NRs [50].

The third work focuses on the electrodeposition of monoclinic bismuth vanadate (BiVO$_4$) on ZnO nanodendrites. Wu et al. have reported an excellent photoanode performance of hierarchical ZnO nanostructure [51]. Furthermore, BiVO$_4$ was selected as the visible light absorber due to its narrow band gap (~2.4 eV), appreciable band edge positions for water oxidation and the matched band structure with that of ZnO [52]. The monoclinic BiVO$_4$ alone demonstrated photocatalytic activity for the O$_2$ evolution from an aqueous silver nitrate solution under visible light illumination [53]. Besides, it has been reported that forming a heterojunction photoanode between the wurtzite ZnO and monoclinic BiVO$_4$ favours the charge separation and transport of electron-hole pairs and promotes a broad range of light absorption [54].

# 3. THE AIMS OF THE DOCTORAL DISSERTATION

This doctoral thesis aims to develop advanced materials to be employed as an efficient photoanode in PEC cells for water-splitting applications. In line with this target, multifunctional ZnO in diverse nanostructures was chosen as a main light absorber in the multi-component nanocomposite systems constructed by three well-documented effective strategies. The specific aims of the doctoral thesis are outlined as follows:

I. Synthesis of ZnO nanorods with three different morphologies by hydrothermal growth using polyethyleneimine as a capping agent was realized. The crystallographic, morphological, and optical properties of the resulting distinct morphologies were characterized by X-ray diffractometer (XRD), scanning electron microscopy (SEM), transmission electron microscopy (TEM), and UV-vis spectroscopy. The impact of morphology on photoanode performance was evaluated by various photoelectrochemical efficiency tests, such as applied bias photon-to-current efficiency (ABPE) and incident photon-to-current conversion efficiency (IPCE).

II. Decoration of Au plasmonic nanoparticles on hydrothermally grown ZnO nanorods was attained by photoreduction synthesis and their gradient doping by subsequent heat treatment as visible light active photoanodes. The above-mentioned typical characterization techniques analyzed the produced heterostructure thin films. The photoanode efficiency of the samples was identified by the general characterization method for PEC application.

III. Growing tiny branches around primarily grown nanorods to fabricate ZnO nanodendrites without any assistance from secondary seeding and its photosensitization with $BiVO_4$ by electrodeposition was accomplished. The type-II heterojunction photoanodes were characterized, and their PEC rankings were determined.

# 4. EXPERIMENTAL

## 4.1 Chemicals and substrate

Zinc acetate dihydrate ($Zn(CH_3CO_2)_2.2H_2O$) was purchased from Penta. Zinc nitrate hexahydrate ($Zn(NO_3)_2 \cdot 6H_2O$), tetrachloroauric(III) acid trihydrate ($HAuCl_4.3H_2O$), bismuth(III) nitrate pentahydrate ($Bi(NO)_3.5H_2O$), ammonium monovanadate ($NH_4VO_3$), and polyethyleneimine (PEI, branched, molecular weight 800), ethylene glycol ($HOCH_2CH_2OH$), dimethyl sulfoxide (DMSO, $(CH_3)_2SO$), and indium tin oxide coated glass substrates (ITO, 5-15 $\Omega.sq^{-1}$) were procured from Sigma Aldrich. Hexamethylenetetramine (HMTA, $(CH_2)6N_4$) and sodium hydroxide (NaOH) were bought from Lachner. Diethanolamine ($(CH_2CH_2OH)_2NH$) was purchased from CDH Fine Chemicals. Isopropanol ($(CH_3)_2CHOH$) was obtained from Microchem. The Milli-Q water purifier supplied deionized water used throughout the experiments (BioPak, Merck, USA). All chemicals were used as received without further purification.

## 4.2 Substrate cleaning

The ITO substrates were cut into square pieces. Prior to the material synthesis, the substrates always underwent ultrasonic cleaning using a solution consisting of alkaline concentrate (Hellmanex III), deionized water, isopropanol, and acetone. Afterwards, they were dried in an atmosphere of air. Eventually, UV-ozone cleaning was employed to eliminate the residual pollutants.

## 4.3 Preparation of ZnO seed layer

The ZnO seed layer was synthesized using a facile sol-gel method. Briefly, the precursor solution was prepared by dissolving 0.036 mol zinc acetate dihydrate and 0,036 mol diethanolamine in 41.5 mL of isopropanol at 50 °C for an hour and aged for 24 h at room temperature. The sol was then spin-coated onto the cleaned ITO substrates at 3000 rpm for 30 s. Finally, the ZnO seed-coated films were calcined at 400 °C in an air atmosphere for 1 h. The same seeding procedure is applied to grow ZnO NRs regardless of the developed heterostructure.

## 4.4 Fabrication of ZnO nanorods with three distinct morphologies by polyethyleneimine

The typical hydrothermal aqueous growth solution, consisting of zinc nitrate hexahydrate and HMTA at equimolar concentrations (0.05 M), was preheated for 2 h at 93 °C in a sealed container. Before the preheating process, 0 mL, 0.50 mL, and 1 mL of PEI were separately added to the above growth solution as a capping agent to evaluate their effects on the nanorods morphology. The addition of PEI resulted in the observed yellow colour change of the solution. The growth solution was found to have a pH value of around 7.1. The ZnO-seeded substrates with conductive surfaces turned upside down were immersed in the heated growth solution. The containers were subjected to a temperature of 93 °C for a duration of 6 h. Following that, the ZnO NRs grown thin films were rinsed with deionized water and dried at 60 °C in an oven. The samples were termed ZnO-P0, ZnO-P0.5, and ZnO-P1 based on the amount of PEI used in their preparation, which was 0 ml, 0.50 ml, and 1 ml, respectively.

## 4.5 Fabrication of Au/ZnO and grad-Au/ZnO heterostructures

### 4.5.1 Preparation of ZnO nanorods

Aqueous growth solution, including equimolar (0.05 M) zinc nitrate hexahydrate and HMTA and PEI (0.50 mL), was preheated for 2 h at 93 °C. The seeded substrates with the conductive faces turned upside down were submersed in this hot solution and maintained at 93 °C for 6 h. The final samples were rinsed with deionized water and dried at 80 °C in an oven.

### 4.5.2 Preparation of Au-sensitized and gradient Au-doped ZnO nanorods

**Fig. 4.1** displays the schematic depiction of the synthesis process of the gradient Au-doped ZnO heterostructure. A simple photoreduction method was used to sensitize Au NPs of ZnO NRs. Aqueous gold salt solution of 10 mM was dissolved in deionized water. The thin films of ZnO nanorods were placed in the solution and exposed to UV radiation from a 365 nm wavelength UV lamp with a power output of 8 W for 1 h. The resulting products were washed with deionized water and dried at 80 °C in an oven. When exposed to light, the formation of a uniform brownish layer shows that gold precursor can be reduced to form Au NPs

on the surface of ZnO. The thin films were then calcined in an air environment at 650 °C for 1 h to induce gradient diffusion of Au NPs into ZnO NRs. The final colour of films became a mottled purple after this process. Hereafter, ZnO NRs, Au-sensitized ZnO NRs, and the gradient Au-doped ZnO NRs will be named ZnO, Au/ZnO and grad-Au/ZnO, respectively.
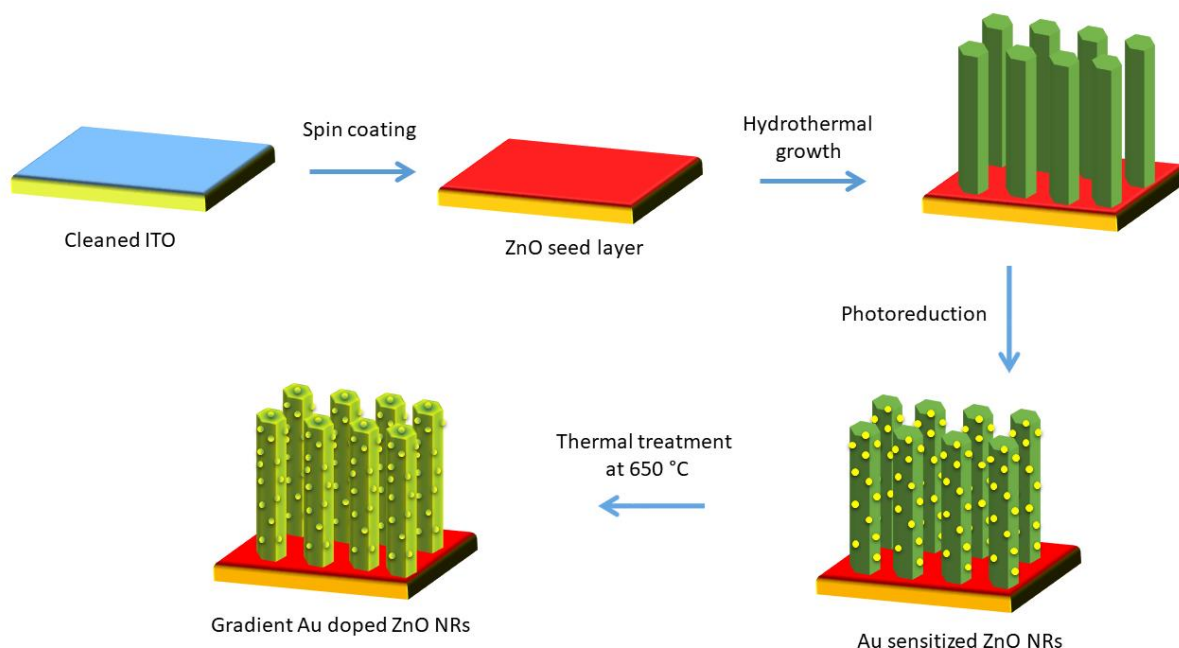


*Fig. 4.1: Schematic depiction of synthesis of gradient Au doped ZnO heterostructure [ACG 2].*

## 4.6 Fabrication of BiVO$_4$/ZnO heterostructure

### 4.6.1 Preparation of ZnO Nanodendrites

The grown ZnO NRs arrays were synthesized by an almost similar hydrothermal procedure described above. 0.025 M zinc nitrate hexahydrate, 0.025 M hexamethylenetetramine, and 0.5 mL PEI were dissolved in deionized water and matured for 2 h at 95 °C. The seeded films, with their conductive side facing downwards, were submerged into the aged growth solution, and kept at 95 °C for 6 h.

The branches of ZnO nanodendrites were formed directly on the ZnO NRs without any assistance from secondary seeding or organic structure-directing agent, as described elsewhere [55]. The ZnO NRs grown on ITO substrate were immersed into an aqueous solution of 0.057 M zinc acetate dihydrate and 0.5 M

NaOH for 20 min at room temperature. During this process, the etch pits develop and act as growth centres for forming the spines on the NRs. After growing in the same solution at 100 °C for 1 h, the spines then turned into branches. The achieved ZnO NDs were thoroughly rinsed with deionized water and dried at 60 °C.

Aqueous zinc acetate and NaOH solution become opaque after being kept at room temperature for 5 minutes, signifying that the solution is supersaturated at room temperature. When ZnO NRs grown substrate is immersed in the already opaque solution, the subsequent hydrothermal process produces only ZnO NWs with slightly increased diameters. It is critical to note that branch development originates from a supersaturated solution in a metastable condition with a high concentration of NaOH. Therefore, it is very important to submerge ZnO NRs in a clear solution before precipitation to develop branches on the surface of NRs.

### 4.6.2 Preparation of BiVO$_4$ and BiVO$_4$/ZnO NDs photoanodes

**Fig. 4.2** presents the synthesis procedure to prepare ZnO NDs coated with BiVO$_4$ NPs, which could be converted from electrodeposited Bi-metal using a modified version of the previously described chemical and thermal treatments [56]. The plating solution was prepared in the first step by dissolving 20 mM of bismuth(III) nitrate pentahydrate in 100 mL ethylene glycol solution.
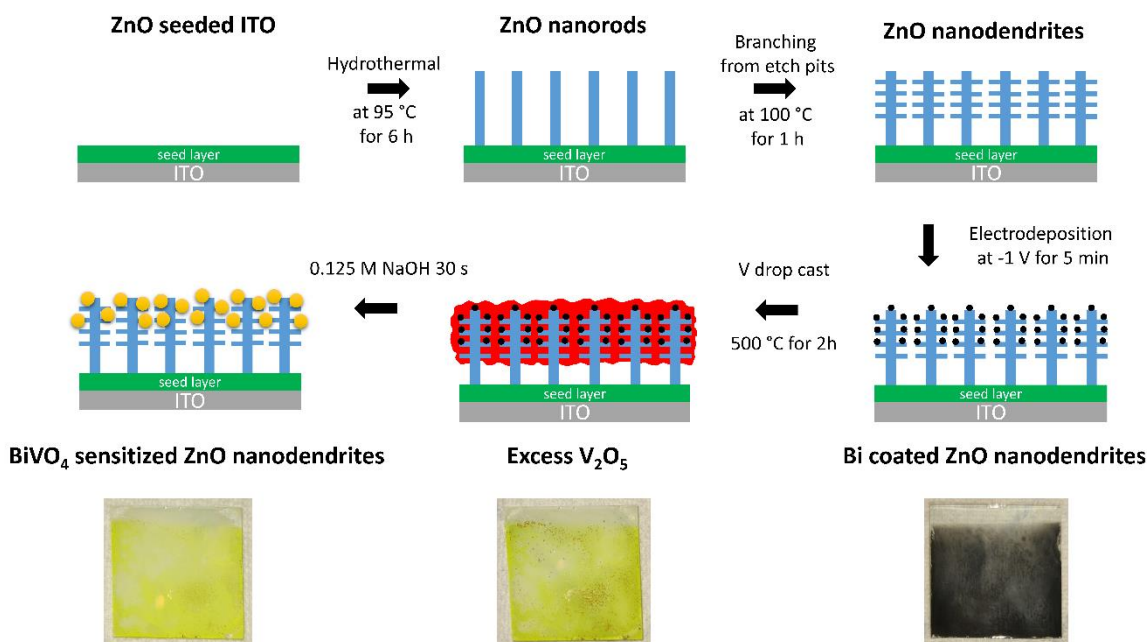


*Fig. 4.2: Schematic representation for the fabrication of BiVO4/ZnO NDs heterojunction photoanode [ACG 3].*

To determine at what voltage the electrodeposition of the Bi-metal start, cyclic voltammogram (CV) of ZnO nanodendrites thin film as a working electrode in a prepared plating solution of Bi was recorded over the potential range from -2 to 2 V vs Ag/AgCl and shown in **Fig. 4.3**.

In CV measurement, the cathodic current linearly increases to -1.1 mA, corresponding to efficient Bi deposition over ZnO NDs electrode. The deposited Bi deoxidizes and strips off the ZnO surface in the reverse scan. The applied potential for Bi deposition was set at -1 V vs Ag/AgCl, where stripping of Bi metal cannot occur. It is also noteworthy that Bi-coated films must be immediately withdrawn from the plating solution as the acidity of this solution is detrimental for Bi deposits, especially when the cathodic protection is no longer prevailing.
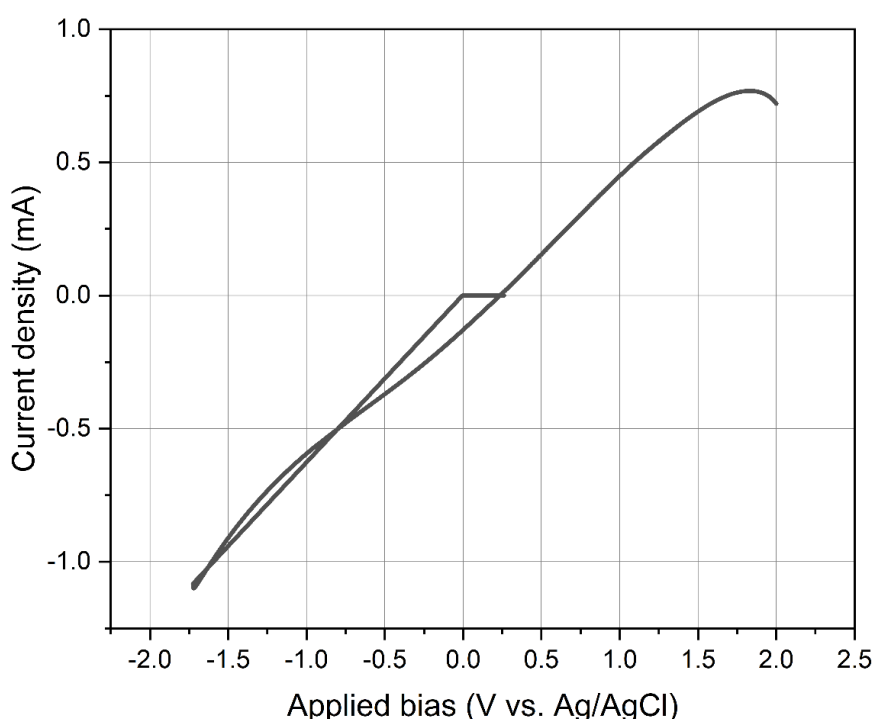


*Fig. 4.3: Cyclic* voltammogram *of ZnO NDs electrode in 100 mL ethylene glycol containing 20 mM bismuth(III) nitrate pentahydrate; bath temperature: 25 °C, solution pH: ~2 [ACG 3].*

The deposition of Bi on ZnO NDs was carried out by passing ~0.033 C/cm$^2$ at -1 V against the Ag/AgCl electrode. Following that, 100 µL of dimethyl sulfoxide containing 150 mM ammonium monovanadate was drop-casted onto the entire Bi film (area = 2 cm$^2$) as the second step. The V precursor-incorporated film was calcined at 500 °C for 2 h in air. By thermal treatment, Bi and VO$^{2+}$ oxidized to Bi$_2$O$_3$ and V$_2$O$_5$, which reacted to form BiVO$_4$. Any residual vanadium pentaoxide

($V_2O_5$) on the electrode was removed by soaking it in 0.125 M NaOH solution for 30 s. The resultant pure $BiVO_4$/ZnO NDs photoanode was thoroughly washed by deionized water and dried at 60 °C. For the synthesis of $BiVO_4$, all the deposition conditions were the same, except for ITO substrates used as scaffolds.

## 4.7 Approaches for PEC efficiency prediction

The incident photocurrent conversion efficiency (IPCE) and the applied bias photon-to-current efficiency (ABPE) measurements are essential for determining the limiting factors of the photoelectrode performance. The IPCE tests were also performed in the three-electrode setup. The IPCE was calculated using the following equation **(4.1)**:

$$IPCE = \frac{J_{ph}(\lambda) \times 1240}{P_{mono}(\lambda) \times \lambda} \tag{4.1}$$

where, $J_{ph}$ (in mA.cm$^{-2}$) is the photocurrent density recorded under monochromatic illumination at wavelength $\lambda$ (in nm), $P_{mono}$ (in mW/cm$^2$) is the light intensity of the monochromatic source at each wavelength, the constant 1240 ($hc/e$ in V.nm) equals the product of Planck's constant and the speed of light divided by the charge of an electron. The ABPE test, analogue to the STH efficiency with no bias, was calculated by the formula **(4.2)**:

$$ABPE = \left[ \frac{J(\text{mA.cm}^{-2}) \times (1.229 - |V_{app}|)(V) \times \eta_F}{P_{total}(\text{mW.cm}^{-2})} \right] \tag{4.2}$$

Here, 1.23 V is the standard state reversible potential for water splitting, $V_{app}$ is the applied bias (measured vs Pt), $\eta_F$ is the Faradaic efficiency for hydrogen evolution ($\eta_F = 1$ in this case), and $P_{total}$ is the light intensity.

## 4.8  Photoelectrochemical and electrochemical measurements

The PEC experiments for evaluating the developed photoanodes throughout the doctoral study were performed in a three-electrode configuration within a plastic cuvette as a PEC cell. The fabricated electrodes with an active surface area of 0.32 cm$^2$, Pt wire and Ag/AgCl (saturated with KCl) were used as the working, counter, and reference electrodes, respectively. 0.5 M Na$_2$SO$_4$ (pH 7) was used as an electrolyte solution that was degassed by nitrogen for 10 min to remove any dissolved oxygen before the PEC measurements. The photoanode was in contact with the electrolyte from the side surface of the cuvette in the direction of incident light, while its bare area was kept outside of the electrolyte to connect with the electrical connection legs. The photoelectrodes were exposed to irradiation from the front side by the light that passed through the electrolyte and cuvette before reaching its surface.

An electrochemical workstation (SP-200 Potentiostat, BioLogic) with Electrochemical Impedance Spectroscopy (EIS) was employed to test the photoelectrochemical/electrochemical performance as well as interfacial charge transfer properties of the produced electrodes. The potentials measured against Ag/AgCl electrode ($E_{Ag/AgCl}$) were converted to NHE potentials ($E_{NHE}$) by using the equation (**4.3**):

$$E_{NHE} = E_{Ag/AgCl} + 0.2 \text{ V} \tag{4.3}$$

The type of light source and electrochemical characterization methods used were implemented according to the electrode/electrolyte interfacial properties and light harvesting capability of the intended material system with the following experimental conditions:

Firstly, ZnO nanorods with three distinct morphologies were front illuminated with a UV light-emitting diode (LED) at 365 nm in all PEC measurements. The net light intensity of ~3 mW.cm$^{-2}$ on the surface of the nanostructured ZnO films was measured with an optical power meter (Opsytec radiometer RM-12). The I-V curves for evaluating the photoelectrochemical performance of the photoanode samples were recorded by the linear sweep voltammetry (LSV) in the potential range from 0.2 V to 1.2 V vs NHE at a scan rate of 20 mV/s. Chronoamperometry (CA, I-t) was conducted to assess photocurrent response in a light on−off cycle under a bias voltage of 0.2 vs NHE. In IPCE measurements, monochromatic LEDs

(Roithner LaserTechnik) were used as monochromatic light sources. The light intensity of LEDs emitting at 365, 390, and 400 nm (close to band edge absorption of ZnO) was measured to be ~3, 0.8 and 0.3 mW.cm$^{-2}$, respectively. Open circuit potential (OCP) of the electrodes was measured under dark and illumination conditions, and 0.1 V window centred at OCP was utilized as the potential range in CV measurements, which were performed in the dark at multiple scan rates within the non-Faradaic potential window to estimate the electrochemical active surface area. In electrochemical impedance spectroscopy measurements (EIS), the impedance spectra were obtained at 10 mV amplitude of AC signal over a frequency range of 100 kHz to 0.1 Hz. The Mott-Schottky (MS) analysis was recorded with 20 potential steps at dark at 1 kHz. Moreover, the photooxidation of $Mn^{+2}$ was also carried out in the three-electrode configuration in 0.5 M $Na_2SO_4$ with 0.01 M $MnSO_4$ under back illumination with the same light source (LED emitting at 365 nm) for 3 min. The deposition was achieved by passing ~0.03 C/cm$^2$ at 0.7 V vs NHE.

Secondly, Au-sensitized and gradient Au-doped ZnO heterostructures were illuminated by the AvaLight-DH-S deuterium halogen source equipped with a fibre optic illuminator with 0.015 mW.cm$^{-2}$ light intensity in the PEC measurements. Moreover, the light was chopped electronically by TTL shutter of light source connected to the potentiostat, which ran the photocurrent experiments at a given period upon external light stimulus (trigger in). In IPCE tests, monochromatic LEDs were used as light sources. LSV curves were recorded by scanning the potential from 0.2 V to 1.2 V vs NHE with a scan rate of 10 mV.s$^{-1}$ in 10 s of light on-off cycles. The CA measurements evaluated the transient photoresponse of the samples under a bias voltage of 0.2 V vs NHE. In EIS measurements, an AC signal of 10 mV amplitude was applied to the cell in the frequency range spanned from 100 kHz to 0.1 Hz. The MS plots were collected in the dark at 1 Hz with 20 potential steps.

Lastly, BiVO$_4$ and BiVO$_4$/ZnO NDs photoanodes were also front side illuminated by a Pico$^{TM}$ solar simulator (G2V Optics) with a standard AM 1.5G filter. The light intensity was 87.8 mW.cm$^{-2}$ at the sample surface. The IPCE tests were carried out using 12 monochromatic channels of the solar simulator (Pico$^{TM}$ with AM 1.5G filter) as the light source. LSV's scan rate was 20 mV.s$^{-1}$, and the scan range was 0.2 V to 1.7 V vs NHE under dark and illuminated conditions. The EIS data under illuminated conditions was obtained at 10 mV amplitude of AC signal over a frequency range of 100 kHz to 0.1 Hz. The MS analysis was carried out in the dark at 1.5 kHz with 30 potential steps.

## 4.9 Characterization

The produced photoanode materials have been characterized to understand their structure and property relationships by following categorized techniques:

1. Crystallographic analysis
   - X-ray diffraction (XRD)
2. Elemental composition analyses
   - X-ray photoelectron spectroscopy (XPS)
   - Energy dispersive X-ray spectroscopy (EDX)
   - Raman spectroscopy
3. Morphology analyses
   - Scanning electron microscope (SEM)
   - Transmission electron microscope (TEM)
4. Optical and physical property analyses
   - UV-vis spectroscopy (UV-vis)
   - Diffuse reflectance spectroscopy (DRS)
   - Photoluminescence Spectroscopy (PL)
   - Kelvin probe force microscope (KPFM) is based on an Atomic Force Microscopy (AFM) setup

# 5. DISCUSSIONS

## 5.1 Comprehensive evaluation of photoelectrochemical performance dependence on geometric feature of ZnO nanorod electrodes

This chapter examines the influence of geometric characteristics, light absorption spectra, and electrochemically active surface area on the photoelectrochemical properties. For this reason, ZnO nanorods with rationally controlled morphologies shown in **Fig. 5.1** were grown on ITO substrates by hydrothermal method and used as a model structure. The dimensions of the nanorods were progressively modified by altering the concentration of polyethyleneimine as a cationic surfactant in the growth solution. The results revealed a strong correlation between the emergent geometric characteristics such as aspect ratio and the electrochemically active surface area. The large surface area and the void space between nanorods increased the photoanode performance by promoting the hole transfer process at the electrode/electrolyte interface. Furthermore, $Mn^{2+}$ as the photogenerated hole imaging agent visually proved that a shorter photogenerated hole diffusion distance leads to improved charge separation efficiency. Therefore, the current work demonstrates an effective strategy of nanorod morphology advancement for creating a strong contact at the electrode/electrolyte interface, which is essential in energy conversion and storage technologies [ACG 1].



✓ *5-fold Aspect ratio*

✓ *+ 20 % Void space between rods*

✓ *+ 40 % Geometric surface area*

✓ *6-fold Electrochem. surface area*

✓ **20-*times Photocurrent density; 0.6 V vs NHE***
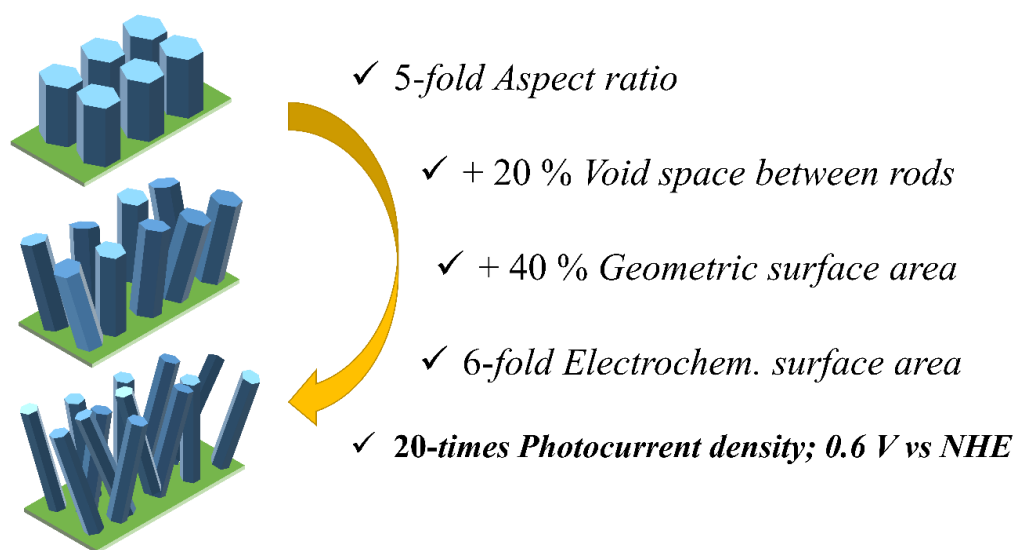
*Fig. 5.1: Schematic illustration of morphology advancement of ZnO NRs and improved geometric features [ACG 1].*

The model structure of ZnO NRs with three different exemplary morphologies was utilized to examine the relationship between surface properties and electrochemical/ photoelectrochemical properties. The geometric features of ZnO NRs grown with the hydrothermal method were progressively modified by varying the PEI amount (0, 0.5 and 1 mL), which inhibited the lateral growth of ZnO crystals. A comprehensive analysis of SEM images enabled the estimation of the crucial surface characteristics of NRs. The aspect ratio and void space of ZnO NRs proportionally increased with increasing PEI concentrations, which correlates with increased specific surface area and the electrochemically available area. The obtained nanostructures with small diameters of ~45 nm demonstrated very effective PEC water-splitting performance. This high PEC activity is addressed to its enhanced electrochemical surface area for more interaction at ZnO/electrolyte interface (interfacial charge kinetics) and enhanced charge collection/separation coming from a shorter photogenerated hole diffusion distance, leading to a more favourable oxygen evolution reaction. Additionally, the scattering effect from internal reflections between randomly orientated tiny NRs in the visible range may contribute to the overall PEC efficiency. The current study anticipates providing comprehensive insight into the correlations between photoelectrochemical characteristics and nanoarchitecture, along with a detailed nanocrystal growth mechanism [ACG 1].

## 5.2 Boosting the photoelectrochemical performance of Au/ZnO nanorods by co-occurring gradient doping and surface plasmon modification

This chapter deals with the band bending modification of metal/semiconductor hybrid nanostructures by gradient doping of Au NPs inwards the ZnO nanorods (NRs) through thermal treatment facilitated faster transport of the photo-induced charge carriers, as depicted in **Fig. 5.2**. Systematic PEC measurements show that the resulting gradient Au-doped ZnO NRs yielded photocurrent density of 0.009 mA.cm$^{-2}$ at 1.1 V (vs NHE), which is 2.5-fold and 8-fold improved than those of Au-sensitized ZnO and the as-prepared ZnO NRs, respectively. The IPCE and ABPE efficiency tests confirmed the boosted photoresponse of gradient Au-incorporated ZnO NRs, particularly in the visible spectrum, due to the synergistic surface plasmonic effect of Au NPs. Gradient Au dopant profile promoted the separation and transfer of the photoinduced charge carriers at the electrolyte interface via more upward band bending according to the elaborated

electrochemical impedance spectroscopy and Kelvin probe force microscopy analyses. Hence, this study introduces a cost-effective and straightforward approach to fabricating semiconductor NRs by incorporating gradient plasmonic noble NPs. These materials exhibit significant potential in the field of energy conversion and storage technologies [ACG 2].
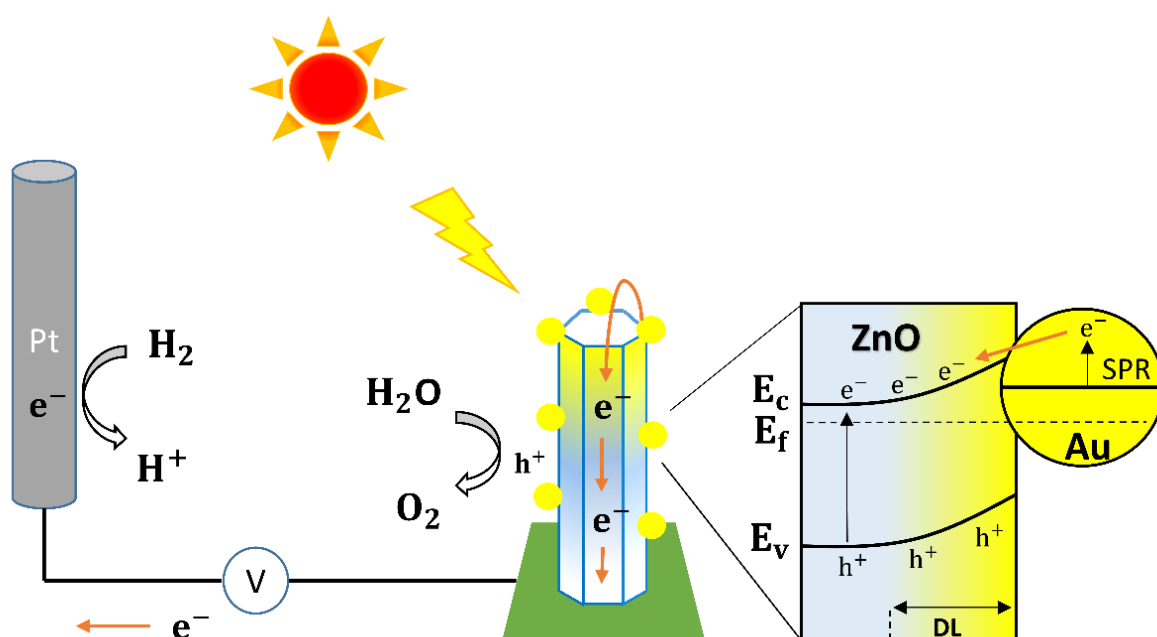


*Fig. 5.2: Schematic depiction of PEC water splitting via grad-Au/ZnO [ACG 2].*

Facile fabrication of efficient ZnO NRs with gradient Au plasmonic NPs incorporation in the radial direction via the hydrothermal technique followed by photoreduction and annealing methods is presented. A promising photocurrent density of 0.009 mA.cm$^{-2}$ at 1.1 V (vs NHE) under 0.015 mW.cm$^{-2}$ light intensity was achieved, which is 2.5-fold and 8-fold improved compared to the Au-sensitized ZnO and the as-prepared ZnO NRs respectively. The EDX line profile analysis verifies that the Au dopant indeed has a gradient concentration profile through the radial direction of the ZnO matrix. The optical spectroscopy techniques, IPCE and ABPE efficiency tests, I-V characteristics as well as the detailed MS and EIS analyses clearly demonstrate that the enhanced PEC performance can be attributed to co-occurring SPR process and charge separation via the formation of more upward band bending of the gradient Au NPs incorporation in the ZnO matrix. The IPCE is three times higher, and ABPE is more than ten times higher for ZnO NRs with gradient Au doping in comparison

with the as-prepared ZnO NRs. Moreover, it is expected that the dual benefit of the plasmonic NPs functionalization as well as their gradient dopant profile, can be expanded to the fabrication of other plasmonic metal NPs and semiconductor heterojunction structures, which are promising in energy conversion and storage technologies [ACG 2].

## 5.3  Nesting BiVO₄ nanoislands in ZnO nanodendrites by two-step electrodeposition for efficient solar water splitting

Photoanodes with a large electrochemically active surface area, rapid charge transfer, and broadband light harvesting capacity are required to maximize the PEC water-splitting performance. To address these features, it is demonstrated that 3D hierarchal ZnO nanodendrites (NDs) can be sensitized with $BiVO_4$ nanoislands by chemical and thermal treatments of electrodeposited Bi-metal films. The flat band measurements and optical characterization suggested that the resulting heterojunction had type-II band alignment with a viable charge transfer from $BiVO_4$ to ZnO NDs, as demonstrated in **Fig. 5.3** [ACG 3].
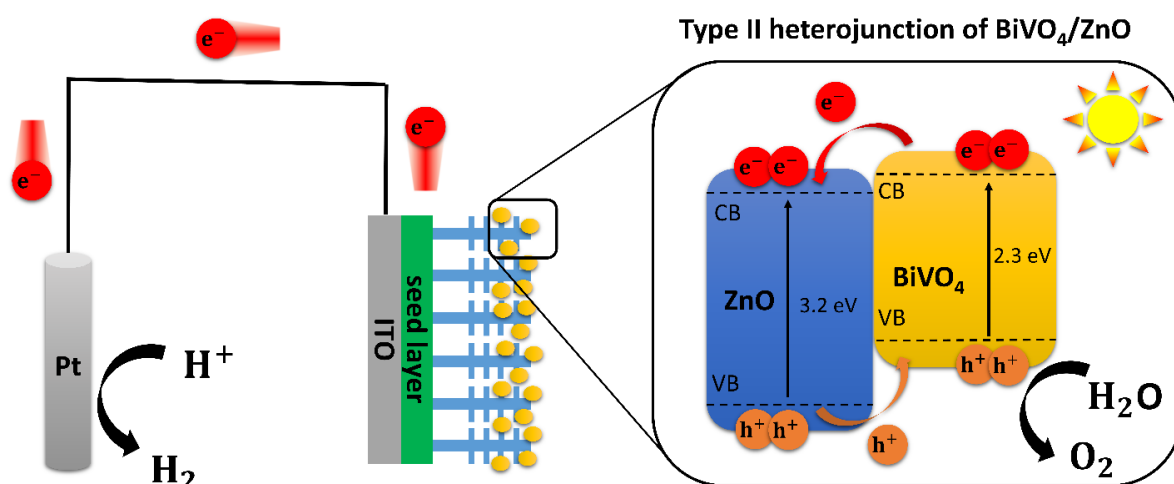


*Fig. 5.3 Photoelectrochemical water splitting mechanism by BiVO₄/ZnO NDs photoanode [ACG 3].*

In parallel, PL analysis revealed inhibition of the charge recombination rate by the electron transfer between $BiVO_4$ and ZnO NDs. Upon AM 1.5G illumination, $BiVO_4$/ZnO NDs heterojunction yielded the highest photocurrent efficiency (0.15 mA.cm$^{-2}$ at 1.2 V vs NHE), which was attributed to its enhanced surface area (due to the presence of small dendrite branches), extended broadband light absorption

extending from UV to visible light regions, and the most efficient interfacial charge transfer as proven by EIS studies. Besides, the IPCE and ABPE tests confirmed an improved spectral photoresponse of the heterojunction-based photoanode, particularly towards the visible light spectrum. The results outline a promising synthesis route for building heterojunctions between visible light active and wide band gap semiconductors for use as highly efficient photoanodes in a PEC cell [ACG 3].

$BiVO_4$/ZnO NDs nanostructure was successfully produced via a facile combination of the hydrothermal method without a secondary seed layer and Bi-metal film electrodeposition followed by the introduction of V precursor solution and thermal treatment. The Bi deposition on ZnO NDs with good adhesion and coverage was achieved after 5 min at -1 V vs Ag/AgCl electrode. It was determined through the flat band and optical measurements that $BiVO_4$/ZnO NDs have type II band alignment, allowing photogenerated electron transfer from $BiVO_4$ to ZnO and vice versa for photogenerated holes. As a result, the $BiVO_4$/ZnO heterojunction photoanode exhibited the highest photocurrent (0.15 $mA.cm^{-2}$ at 1.2 V vs NHE), which is 1.5, 2.5 and 5 times higher than that of ZnO NDs, $BiVO_4$, ZnO NRs photoanodes produced in this study. The significant advancement in photocurrent efficiency of the heterojunction photoanode produced in this study was associated with several factors: 1) enhanced light absorption towards the visible light region (due to narrow band gap of 2.3 eV for $BiVO_4$); 2) favourable charge transfer confirmed by lower interfacial charge transfer resistance (thinner branches around NRs endows stronger contact area between electrode/electrolyte); 3) suppression of charge recombination rate, thus more efficient charge separation. The electrodeposition of the primary metal layer to convert into visible light absorber material is feasible to sensitize photoanode materials with poor light absorption. The current work can be expanded to fabricate various highly efficient heterostructured photoanodes for use in PEC water splitting and other solar energy applications [ACG 3].

# 6. CONCLUSIONS, REMARKS, AND FUTURE PERSPECTIVES

## 6.1 Summary of accomplishments based on defined research objectives

This thesis focuses on the fabrication of novel photoanode materials with high efficiency for potential applications in PEC water splitting. The steps required to attain the aim mentioned above are presented in a concise manner as follows:

- The fundamental considerations in selecting photoanode materials in a PEC cell included a thermodynamic requirement, appropriate band gap and band edge positions, high surface area, high stability and low-cost. ZnO with UV light absorption ability was sensitized by visible light absorbers $BiVO_4$ and Au nanoparticles to improve PEC performance.

- As a result of a thorough relevant literature review, well-established and facile chemical synthesis methods were utilized for the development of determined materials, specifically hydrothermal method for ZnO NRs with three distinct morphologies, photoreduction method for grad-Au/ZnO and electrodeposition of $BiVO_4$. The utility of these approaches produced thin films with good coverage, adhesion, and electrical continuity. Fabricating dense Bi thin film electrodes remains a major challenge due to the poor solubility of Bi(III) containing salts unless the solution is strongly acidic. This leads to corrosion of the main layer to be deposited after 5 min of electrodeposition operation duration, not allowing good control over deposition thickness.

- Novel strategies were adopted to modify the resulting metal oxide thin films for enhanced PEC efficiency. The morphology of the synthesized high aspect-ratio NRs was systematically studied, and their distinct surface features were estimated. Noble plasmonic metal (Au) decoration and its gradient doping profile were simultaneously used to benefit from the phenomenological surface plasmon effect and more upward band bending at the metal/semiconductor interface. Furthermore, a heterostructure between wide band gap ZnO and narrow band gap $BiVO_4$ was constructed to extend light-harvesting capacity. The formation of type-II heterojunction that is sensitive to visible light was successfully identified.

- All these advanced systems were characterized by cutting-edge techniques and studied for accurate evaluation for use in PEC water splitting.

- The experimental data and results obtained in this dissertation have been published in a high-ranking journal with a Q1/Q2 impact factor, in compliance with the University Policy and the rector's directive.

## 6.2 Summary of research outputs

An overview of the research outputs that have already been published and under journal communication in the doctoral thesis is presented:

**Main theme of the research in section 5.1**: Construction of ZnO NRs with different nanoarchitecture designs to understand the correlation between morphology and photoelectrochemical activity.

This study investigates the morphology dependency of PEC water splitting to achieve a highly efficient photoanode material. ZnO NRs with three different morphologies were prepared with the help of polyethyleneimine as a crystal growth inhibitor. The concentration of cationic surface-active agent in the hydrothermal growth was optimized, and the threshold value was progressively determined. It was found that increasing surfactant concentration progressively yielded thinner and longer ZnO NRs. The increase in aspect-ratio was proportional to the increase in the electrochemical active surface area. The PEC performance of the produced samples was studied by UV light-emitting diode used as a light source. ZnO-P1 with superior surface characteristics exhibited the highest photocurrent value. Moreover, $Mn^{2+}$ as the photogenerated hole imaging agent was utilized to identify hole extraction pathways depending on different nanorod`s dimensions. A strong correlation was found between the emerging geometric properties and the PEC activity of the electrodes. The obtained results indicate that rational control over NRs morphology can effectively enhance the PEC performance.

The core of this work topic has been published in *Nanoscale Advances* with a title of "Comprehensive evaluation of photoelectrochemical performance dependence on geometric features of ZnO nanorod electrodes".

Author contribution: Investigation, conceptualization, methodology, writing and editing original draft preparation.

**Main theme of the research in section 5.2**: The concurrent utilization of Au plasmonic nanoparticles and their gradient doping to make ZnO NRs superior visible light active photoanode material.

This research describes the fabrication of ZnO NRs arrays modified with controlled Au surface doping by a facile photoreduction method followed by thermal treatment and its use as a photoanode for PEC water splitting under illumination. A gradient distribution of Au dopants along the radial direction of ZnO NRs was realized. Grad-Au/ZnO exhibited a markedly enhanced PEC photocurrent density compared to Au/ZnO and pristine ZnO. The gradient Au dopant profile not only actuated visible light absorption ability but also introduced upward band bending due to terrace-like band structure, which blocks the back electron transfer and promotes charge separation efficiency. Consequently, incorporating gradient plasmonic noble metal NPs inwards ZnO NRs has promising potential in energy conversion applications.

The core of this work topic has been published in *International Journal of Molecular Sciences* with a title of "Boosting the Photoelectrochemical Performance of Au/ZnO Nanorods by Co-Occurring Gradient Doping and Surface Plasmon Modification".

Author contribution: Investigation, conceptualization, methodology, writing and editing original draft preparation.

**Main theme of the research in section 5.3**: Structural evolution from nanorods to nanodendrites and photosensitization by visible light absorbing $BiVO_4$ to achieve high PEC efficiency.

This study aimed to produce a photoanode with a large electrochemically active surface area and broadband light absorption capacity. It is revealed that $BiVO_4$ NPs were decorated on ZnO NDs by electrodeposition followed by chemical and thermal treatments. $BiVO_4$/ZnO NDs heterostructure generated the maximum photocurrent efficiency because of enlarged surface area and extended optical light absorption edge to visible light region. This heterojunction was determined to have type-II band alignment with a viable electron transfer from $BiVO_4$ to ZnO. The superior potential of the primarily deposited metal layer for converting visible light absorber material on the host semiconductor will provide novel insights into heterojunction photoelectrode for solar water splitting.

The core of this work topic has been turned into a manuscript and *under journal communication* with a title of *"Nesting BiVO4 nanoislands in ZnO nanodendrites by two-step electrodeposition for efficient solar water splitting"*.

Author contribution: Investigation, conceptualization, methodology, writing and editing original draft preparation.

## 6.3 Contribution to science and future prospects

The research outlined in this thesis offers original contributions to photoelectrochemical water splitting, an area of significant interest in renewable energy research. These contributions can be categorized into scientific perspective, practical implications, and guidance for future research.

This research enriches the scientific discussion by providing detailed studies on material properties, synthesis methods, and structural modifications of selected semiconducting materials. The primary aim of this doctoral dissertation was the development of novel and highly efficient photoanode materials for photoelectrochemical water splitting, particularly ZnO, sensitized with BiVO4 and Au nanoparticles. A significant scientific contribution is the exploration of how modifications to thin metal oxide films, such as morphological parameters, hierarchical structure, gradient doping, and heterostructure formation, impact light absorption and charge separation. This objective was successfully fulfilled by the fabrication of advanced hybrid photoanode materials with various effective strategies in sections 5.2 and 5.3. Moreover, the work in section 5.1 has covered a comprehensive study on the morphological dependence of PEC water splitting.

The applicability of this research is most evident in its potential to enhance the efficiency of PEC water splitting. The produced materials were able to catalytically convert photons from sunlight into chemical energy, which is a key to sustainable energy solutions in solar-to-hydrogen conversion technologies. This research broadens the scope of materials utilized in renewable energy technologies by demonstrating the effectiveness of sensitized ZnO and other modified materials in PEC systems. These materials employed in PEC cells for PEC water splitting were robust in the aqueous electrolyte solution despite otherwise inevitable photocorrosion at high applied potentials and intense light intensity.

It should be noted that experiments in the context of this thesis work have been implemented and limited to a small-scale application and, therefore, cannot respond to the needs of commercial usage on a large scale today. Nevertheless, the methodologies and findings presented in this thesis can guide future research in the field. The approaches and solutions offered for material challenges in this work provide a blueprint for subsequent studies aiming to improve the efficiency and practicality of PEC systems, particularly in subsequent research aiming to optimize the enhancement of photoanode materials further, particularly in the area of nanostructure optimization and surface modification for energy applications.

The increasing energy demand with the increasing population is swiftly depleting our current resources. This means taking greater advantage of renewable energy fuels to address the gap in energy needs. If PEC cells are intended to be key to increasing the use of solar energy in total energy production, there is a need to decrease the cost of electrode materials. Furthermore, in the direction of the emerging research areas, the prospective targets for advancing photoelectrochemical technologies can involve 1) enhancing the efficiency of stable materials, 2) enhancing the stability of efficient materials, and 3) exploring new materials that are intrinsically stable and high efficiency. May the research work carried out within the scope of this thesis will contribute to the field of PEC water splitting, at least to some extent. With this, PEC cells will hopefully be integrated into our lives soon.

# REFERENCES

**Author's works**

[ACG 1] A.C. Guler, J. Antos, M. Masar, M. Machovsky, I. Kuritka, M. Urbanek, Comprehensive evaluation of photoelectrochemical performance dependence on geometric features of ZnO nanorod electrodes †, (2023). https://doi.org/10.1039/d3na00089c.

[ACG 2] A.C. Güler, J. Antoš, M. Masař, M. Urbánek, M. Machovský, I. Kuřitka, Boosting the Photoelectrochemical Performance of Au/ZnO Nanorods by Co-Occurring Gradient Doping and Surface Plasmon Modification, Int. J. Mol. Sci. 24 (2023). https://doi.org/10.3390/ijms24010443.

[ACG 3] A.C. Guler, J. Antos, M. Masar, M. Urbanek, M. Machovsky, R. Dagupati, M. Zitnan, J.J. Velazquez, D. Galusek, I. Kuritka, Nesting $BiVO_4$ nanoislands in ZnO nanodendrites by two-step electrodeposition for efficient solar water splitting (under journal communication)".

**Other references**

[1]  A.I. Osman, L. Chen, M. Yang, G. Msigwa, M. Farghali, S. Fawzy, D.W. Rooney, P.S. Yap, Cost, environmental impact, and resilience of renewable energy under a changing climate: a review, Environ. Chem. Lett. 21 (2023) 741–764. https://doi.org/10.1007/s10311-022-01532-8.

[2]  S. Shafiee, E. Topal, When will fossil fuel reserves be diminished?, Energy Policy. 37 (2009) 181–189. https://doi.org/10.1016/j.enpol.2008.08.016.

[3]  Y.J. Zhang, Z. Liu, H. Zhang, T. De Tan, The impact of economic growth, industrial structure and urbanization on carbon emission intensity in China, Nat. Hazards. 73 (2014) 579–595. https://doi.org/10.1007/s11069-014-1091-x.

[4]  D. Gielen, F. Boshell, D. Saygin, M.D. Bazilian, N. Wagner, R. Gorini, The role of renewable energy in the global energy transformation, Energy Strateg. Rev. 24 (2019) 38–50. https://doi.org/10.1016/j.esr.2019.01.006.

[5]  European Commission, European Climate Law, Off. J. Eur. Union. 2021 (2021) 17. https://eur-lex.europa.eu/legal-content/EN/TXT/?uri=CELEX:32021R1119.

[6]  G. Tanil, P. Jurek, Policies on renewable energy at the European and national level of governance: Assessing policy adaptation in the Czech Republic, Energy Reports. 6 (2020) 548–553.

https://doi.org/10.1016/j.egyr.2019.09.024.

[7]  O. Edenhofer, R.P. Madruga, Y. Sokona, K. Seyboth, P. Matschoss, S. Kadner, T. Zwickel, P. Eickemeier, G. Hansen, S. Schlömer, C. von Stechow, Renewable energy sources and climate change mitigation: Special report of the intergovernmental panel on climate change, 2011. https://doi.org/10.1017/CBO9781139151153.

[8]  L.I.M. Asri, W.N.S.F.W. Ariffin, A.S.M. Zain, J. Nordin, N.S. Saad, Comparative Study of Energy Storage Systems (ESSs), J. Phys. Conf. Ser. 1962 (2021). https://doi.org/10.1088/1742-6596/1962/1/012035.

[9]  H. Ibrahim, A. Ilinca, J. Perron, Energy storage systems-Characteristics and comparisons, Renew. Sustain. Energy Rev. 12 (2008) 1221–1250. https://doi.org/10.1016/j.rser.2007.01.023.

[10]  I.R. Barba, Investigations into electrochemical water splitting, Thesis. (2017).

[11]  J. Jia, L.C. Seitz, J.D. Benck, Y. Huo, Y. Chen, J.W.D. Ng, T. Bilir, J.S. Harris, T.F. Jaramillo, Solar water splitting by photovoltaic-electrolysis with a solar-to-hydrogen efficiency over 30%, Nat. Commun. 7 (2016) 1–6. https://doi.org/10.1038/ncomms13237.

[12]  A. Fujishima, K. Honda, Electrochemical photolysis of water at a semiconductor electrode., Nature. 238 (1972) 37–38. https://doi.org/10.1038/238037a0.

[13]  K.W. Harrison, Remick R., G.D. Martin, A. Hoskin, Hydrogen Production: Fundamentals and Case Study Summaries, Hydrog. Fuel Cells. (2010) 207–226.

[14]  C. Lamy, P. Millet, A critical review on the definitions used to calculate the energy efficiency coefficients of water electrolysis cells working under near ambient temperature conditions, J. Power Sources. 447 (2020) 227350. https://doi.org/10.1016/j.jpowsour.2019.227350.

[15]  M.A. Marwat, M. Humayun, M.W. Afridi, H. Zhang, M.R. Abdul Karim, M. Ashtar, M. Usman, S. Waqar, H. Ullah, C. Wang, W. Luo, Advanced Catalysts for Photoelectrochemical Water Splitting, ACS Appl. Energy Mater. 4 (2021) 12007–12031. https://doi.org/10.1021/acsaem.1c02548.

[16]  E. Kalamaras, M. Mercedes Maroto-Valer, J.M. Andresen, H. Wang, J. Xuan, Thermodynamic analysis of the efficiency of photoelectrochemical CO2 reduction to ethanol, Energy Procedia. 158 (2019) 767–772. https://doi.org/10.1016/j.egypro.2019.01.204.

[17]  R.T. Tung, Recent advances in Schottky barrier concepts, Mater. Sci. Eng. R Reports. 35 (2001) 1–138. https://doi.org/10.1016/S0927-796X(01)00037-7.

[18]  J. Gan, X. Lu, Y. Tong, Towards highly efficient photoanodes: Boosting sunlight-driven semiconductor nanomaterials for water oxidation, Nanoscale. 6 (2014) 7142–7164. https://doi.org/10.1039/c4nr01181c.

[19]  A.G. Tamirat, J. Rick, A.A. Dubale, W.N. Su, B.J. Hwang, Using hematite

for photoelectrochemical water splitting: A review of current progress and challenges, Nanoscale Horizons. 1 (2016) 243–267. https://doi.org/10.1039/c5nh00098j.

[20] K. Kumar, M. Chitkara, I.S. Sandhu, D. Mehta, S. Kumar, Photocatalytic, optical and magnetic properties of Fe-doped ZnO nanoparticles prepared by chemical route, J. Alloys Compd. 588 (2014) 681–689. https://doi.org/10.1016/j.jallcom.2013.11.127.

[21] S. Zaman, Synthesis of ZnO, CuO and their Composite Nanostructures for Optoelectronics, Sensing and Catalytic Applications, Sweden, 2012.

[22] H. Morkoc, U. Ozgur, General Properties of ZnO, 2009. https://doi.org/10.1002/9783527623945.ch1.

[23] S.-C. Liu, J.-J. Wu, Low-temperature and catalyst-free synthesis of well-aligned ZnO nanorods on Si (100), J. Mater. Chem. 12 (2002) 3125–3129. https://doi.org/10.1039/b203871d.

[24] M.A. Mahmood, S. Jan, I.A. Shah, I. Khan, Growth Parameters for Films of Hydrothermally Synthesized One-Dimensional Nanocrystals of Zinc Oxide, Int. J. Photoenergy. 2016 (2016). https://doi.org/10.1155/2016/3153170.

[25] Y. Yang, S. Niu, D. Han, T. Liu, G. Wang, Y. Li, Progress in Developing Metal Oxide Nanomaterials for Photoelectrochemical Water Splitting, Adv. Energy Mater. 7 (2017) 1–26. https://doi.org/10.1002/aenm.201700555.

[26] M. Ma, Y. Huang, J. Liu, K. Liu, Z. Wang, C. Zhao, S. Qu, Z. Wang, Engineering the photoelectrochemical behaviors of ZnO for efficient solar water splitting, J. Semicond. 41 (2020). https://doi.org/10.1088/1674-4926/41/9/091702.

[27] C. Chen, W. Yu, T. Liu, S. Cao, Y. Tsang, Graphene oxide/WS2/Mg-doped ZnO nanocomposites for solar-light catalytic and anti-bacterial applications, Sol. Energy Mater. Sol. Cells. 160 (2017) 43–53. https://doi.org/10.1016/j.solmat.2016.10.020.

[28] Z.L. Wang, Nanostructures of zinc oxide, Int. J. Nanotechnol. 6 (2009) 245–257. https://doi.org/10.1504/IJNT.2009.022917.

[29] Y. Qiu, K. Yan, H. Deng, S. Yang, Secondary branching and nitrogen doping of ZnO nanotetrapods: Building a highly active network for photoelectrochemical water splitting, Nano Lett. 12 (2012) 407–413. https://doi.org/10.1021/nl2037326.

[30] S.H. Ko, D. Lee, H.W. Kang, K.H. Nam, J.Y. Yeo, S.J. Hong, C.P. Grigoropoulos, H.J. Sung, Nanoforest of hydrothermally grown hierarchical ZnO nanowires for a high efficiency dye-sensitized solar cell, Nano Lett. 11 (2011) 666–671. https://doi.org/10.1021/nl1037962.

[31] A.I. Hochbaum, P. Yang, Semiconductor Nanowires for Energy Harvesting, Semicond. Semimetals. 94 (2016) 297–368. https://doi.org/10.1016/bs.semsem.2015.09.001.

[32] T.L. Sounart, J. Liu, J.A. Voigt, J.W.P. Hsu, E.D. Spoerke, Z. Tian, Y. Jiang, Sequential nucleation and growth of complex nanostructured films, Adv. Funct. Mater. 16 (2006) 335–344. https://doi.org/10.1002/adfm.200500468.

[33] L. Goswami, N. Aggarwal, R. Verma, S. Bishnoi, S. Husale, R. Pandey, G. Gupta, Graphene Quantum Dot-Sensitized ZnO-Nanorod/GaN-Nanotower Heterostructure-Based High-Performance UV Photodetectors, ACS Appl. Mater. Interfaces. 12 (2020) 47038–47047. https://doi.org/10.1021/acsami.0c14246.

[34] S. Chabri, A. Dhara, B. Show, D. Adak, A. Sinha, N. Mukherjee, Mesoporous CuO-ZnO p-n heterojunction based nanocomposites with high specific surface area for enhanced photocatalysis and electrochemical sensing, Catal. Sci. Technol. 6 (2016) 3238–3252. https://doi.org/10.1039/c5cy01573a.

[35] D. Wu, J. Tian, Y. Xing, X. Jin, G. Ni, Fabrication of Z-scheme ZnO/Bi2O4 heterojunction photocatalyst with superior photocatalytic nitrogen fixation under visible light irradiation, Solid State Sci. 119 (2021) 106709. https://doi.org/10.1016/j.solidstatesciences.2021.106709.

[36] K.R. Nandanapalli, D. Mudusu, Surface Passivated Zinc Oxide (ZnO) Nanorods by Atomic Layer Deposition of Ultrathin ZnO Layers for Energy Device Applications, ACS Appl. Nano Mater. 1 (2018) 4083–4091. https://doi.org/10.1021/acsanm.8b00816.

[37] S. Bai, S. Jia, Y. Zhao, Y. Feng, R. Luo, D. Li, A. Chen, NiFePB-modified ZnO/BiVO4 photoanode for PEC water oxidation, Dalt. Trans. (2023) 5760–5770. https://doi.org/10.1039/d3dt00013c.

[38] I. Grigioni, G. Di Liberto, M.V. Dozzi, S. Tosoni, G. Pacchioni, E. Selli, WO3/BiVO4Photoanodes: Facets Matching at the Heterojunction and BiVO4Layer Thickness Effects, ACS Appl. Energy Mater. 4 (2021) 8421–8431. https://doi.org/10.1021/acsaem.1c01623.

[39] S. Li, W. Xu, L. Meng, W. Tian, L. Li, Recent Progress on Semiconductor Heterojunction-Based Photoanodes for Photoelectrochemical Water Splitting, Small Sci. 2 (2022). https://doi.org/10.1002/smsc.202100112.

[40] J. Liu, H. He, D. Xiao, S. Yin, W. Ji, S. Jiang, D. Luo, B. Wang, Y. Liu, Recent advances of plasmonic nanoparticles and their applications, Materials (Basel). 11 (2018). https://doi.org/10.3390/ma11101833.

[41] J.C. Phys, Plasmonic hot electrons for sensing , photodetection , and solar energy applications : A perspective Plasmonic hot electrons for sensing , photodetection , and solar energy applications : A perspective, 220901 (2020). https://doi.org/10.1063/5.0005334.

[42] M. Janczarek, E. Kowalska, On the origin of enhanced photocatalytic activity of copper-modified titania in the oxidative reaction systems, Catalysts. 7 (2017). https://doi.org/10.3390/catal7110317.

[43] F.F. Abdi, L. Han, A.H.M. Smets, M. Zeman, B. Dam, R. Van De Krol,

Efficient solar water splitting by enhanced charge separation in a bismuth vanadate-silicon tandem photoelectrode, Nat. Commun. 4 (2013) 1–7. https://doi.org/10.1038/ncomms3195.

[44] F. Feng, C. Li, J. Jian, F. Li, Y. Xu, H. Wang, L. Jia, Gradient Ti-doping in hematite photoanodes for enhanced photoelectrochemical performance, J. Power Sources. 449 (2020) 227473. https://doi.org/10.1016/j.jpowsour.2019.227473.

[45] Kuanfei Liu, W. Wu, B. Chen, X. Chen, N. Zhang, Continuous Growth and Improved PL Property of ZnO Nanoarrays with Assistance of Polyethylenimine, Nanoscale. (2013). https://doi.org/DOI https://doi.org/10.1039/C3NR00559C.

[46] Y. Zhou, W. Wu, G. Hu, H. Wu, S. Cui, Hydrothermal synthesis of ZnO nanorod arrays with the addition of polyethyleneimine, Mater. Res. Bull. 43 (2008) 2113–2118. https://doi.org/10.1016/j.materresbull.2007.09.024.

[47] X. Sun, Q. Li, J. Jiang, Y. Mao, Morphology-tunable synthesis of ZnO nanoforest and its photoelectrochemical performance, Nanoscale. 6 (2014) 8769–8780. https://doi.org/10.1039/c4nr01146e.

[48] H.M.E. Azzazy, M.M.H. Mansour, T.M. Samir, R. Franco, Gold nanoparticles in the clinical laboratory: Principles of preparation and applications, Clin. Chem. Lab. Med. 50 (2012) 193–209. https://doi.org/10.1515/cclm.2011.732.

[49] M.A. Desai, V. Sharma, M. Prasad, G. Gund, S. Jadkar, S.D. Sartale, Photoelectrochemical performance of MWCNT–Ag–ZnO ternary hybrid: a study of Ag loading and MWCNT garnishing, J. Mater. Sci. 56 (2021) 8627–8642. https://doi.org/10.1007/s10853-021-05821-5.

[50] C.W. Cheng, E.J. Sie, B. Liu, C.H.A. Huan, T.C. Sum, H.D. Sun, H.J. Fan, Surface plasmon enhanced band edge luminescence of ZnO nanorods by capping Au nanoparticles, Appl. Phys. Lett. 96 (2010) 3–5. https://doi.org/10.1063/1.3323091.

[51] C. Te Wu, W.P. Liao, J.J. Wu, Three-dimensional ZnO nanodendrite/nanoparticle composite solar cells, J. Mater. Chem. 21 (2011) 2871–2876. https://doi.org/10.1039/c0jm03481a.

[52] Y. Bai, J. Lu, H. Bai, Z. Fang, F. Wang, Y. Liu, D. Sun, B. Luo, W. Fan, W. Shi, Understanding the key role of vanadium in p-type BiVO 4 for photoelectrochemical N 2 fixation, Chem. Eng. J. 414 (2021) 128773. https://doi.org/10.1016/j.cej.2021.128773.

[53] A. Kudo, K. Omori, H. Kato, A novel aqueous process for preparation of crystal form-controlled and highly crystalline BiVO4 powder from layered vanadates at room temperature and its photocatalytic and photophysical properties, J. Am. Chem. Soc. 121 (1999) 11459–11467. https://doi.org/10.1021/ja992541y.

[54] H.T. Wang, J.W. Chiou, K.H. Chen, A.R. Shelke, C.L. Dong, C.H. Lai, P.H. Yeh, C.H. Du, C.Y. Lai, K. Asokan, S.H. Hsieh, H.W. Shiu, C.W.

Pao, H.M. Tsai, J.S. Yang, J.J. Wu, T. Ohigashi, W.F. Pong, Role of Interfacial Defects in Photoelectrochemical Properties of BiVO4Coated on ZnO Nanodendrites: X-ray Spectroscopic and Microscopic Investigation, ACS Appl. Mater. Interfaces. 13 (2021) 41524–41536. https://doi.org/10.1021/acsami.1c08522.

[55] C. Te Wu, J.J. Wu, Room-temperature synthesis of hierarchical nanostructures on ZnO nanowire anodes for dye-sensitized solar cells, J. Mater. Chem. 21 (2011) 13605–13610. https://doi.org/10.1039/c1jm11681a.

[56] D. Kang, Y. Park, J.C. Hill, K. Choi, Preparation of Bi-Based Ternary Oxide Photoanodes BiVO4,Bi2WO6, and Bi2Mo3O12 Using Dendritic Bi Metal Electrodes, J. Phys. Chem. Lett. (2014) 2994–2999. https://doi.org/dx.doi.org/10.1021/jz501544k.

# LIST OF FIGURES

# LIST OF ABBREVIATIONS AND SYMBOLS

| | |
|---|---|
| PEC | Photoelectrochemical |
| OER | Oxygen evolution reaction |
| HER | Hydrogen evolution reaction |
| STH | Solar to hydrogen |
| NHE | Normal hydrogen electrode |
| ITO | Indium doped tin oxide |
| VB | Valence band |
| CB | Conduction band |
| SPR | Surface plasmon resonance |
| PEI | Polyethyleneimine |
| IPCE | Incident photon to current conversion efficiency |
| ABPE | Applied bias photon-to-current efficiency |
| NRs | Nanorods |
| NPs | Nanoparticles |
| NDs | Nanodendrites |
| ZnO | Zinc oxide |
| $BiVO_4$ | Bismuth vanadate |
| XRD | X-ray diffraction |
| SEM | Scanning electron microscopy |
| PL | Photoluminescence |
| NBE | Near band emission |

# Curriculum vitae

| | |
|---|---|
| Name: | Ali Can GULER |
| Date of birth: | 23/07/1991 |
| Place of birth: | Adana, Turkey |
| Permanent address: | İnönü caddesi erden apartmanı 25/3 Marmaris/Turkey. |
| Affiliation: | Centre of Polymer Systems, Tomas Bata University in Zlin, 76001 Zlin, Czech Republic. |
| E-mail: | guler@utb.cz |
| Education: | **2019 – to date** |

**2019 – to date**

Ph.D. studies in Nanotechnology and advanced Materials, Center of Polymer Systems, Tomas Bata University in Zlin, Czech Republic.

**2015 – 2017**

Master of science in Material Science and Engineering, Ege University, İzmir, Turkey.

**2010 – 2015**

Bachelor of Science in Physics, Ege University - İzmir, Turkey.

## External funding:

i.  **Research Project staff (2019 – to date):** LTT20010 – "Concept of heterostructured nanoparticles inspired by artificial photosynthesis".

## Internal funding:

i.  **Member of the research team (2023):** IGA/CPS/2023/006 – "Preparation and characterization of advanced functional nanocomposite systems".

**List of Publications**

**First Authored Contributions:**

1. **A. C. Güler**, J. Antos, M. Masar, M. Machovsky, I. Kuritka, and M. Urbanek, "Comprehensive evaluation of photoelectrochemical performance dependence on geometric features of ZnO nanorod electrodes," 2023.
2. **A. C. Güler**, J. Antoš, M. Masař, M. Urbánek, M. Machovský, and I. Kuřitka, "Boosting the Photoelectrochemical Performance of Au/ZnO Nanorods by Co-Occurring Gradient Doping and Surface Plasmon Modification," *Int. J. Mol. Sci.*, vol. 24, no. 1, 2023.
3. B. Dindar and **A. C. Güler**, "Comparison of facile synthesized N doped, B doped and undoped ZnO for the photocatalytic removal of Rhodamine B," *Environ. Nanotechnology, Monit. Manag.*, vol. 10, no. September, pp. 457–466, 2018.
4. **A. C. Güler**, B. Dindar, and H. Orücü, "Effect of B or N doping on the dielectric and electrical properties of ZnO at room temperature," *Mater. Res. Express*, vol. 6, no. 6, 2019.
5. **A.C. Guler**, J. Antos, M. Masar, M. Urbanek, M. Machovsky, R. Dagupati, M. Zitnan, J.J. Velazquez, D. Galusek, I. Kuritka, "Nesting BiVO$_4$ nanoislands in ZnO nanodendrites by two-step electrodeposition for efficient solar water splitting (under journal communication)".

**Co-Authored Contributions:**

1. M. Masar *et al.*, "Multifunctional bandgap-reduced ZnO nanocrystals for photocatalysis, self-cleaning, and antibacterial glass surfaces," *Colloids Surfaces A Physicochem. Eng. Asp.*, vol. 656, no. PA, p. 130447, 2023.
2. H. Ali, M. Masar, A. C. Guler, M. Urbanek, M. Machovsky, and I. Kuritka, "Heterojunction-based photocatalytic nitrogen fixation: principles and current progress," *Nanoscale Adv.*, vol. 3, no. 22, pp. 6358–6372, 2021.
3. H. Ali *et al.*, "Solid-state synthesis of direct z-scheme cu2o/wo3 nanocomposites with enhanced visible-light photocatalytic performance," *Catalysts*, vol. 11, no. 2, pp. 1–26, 2021.

**Conference Contributions:**

1. 3rd National Environmental Conference, "Photodegradation of Organic Contaminants by Modified Metal Oxide Nanoparticles", 24-28 Sep 2016, Marmaris, Turkey.

2. 5th International Conference on Applied Surface Science, "Role of Polyethyleneimine on the crystal orientation of ZnO nanorods for photoelectrochemical water splitting", 25-28 Apr 2022, Palma, Mallorca, Spain.
3. 25th International Symposium on the Photochemistry and Photophysics of Coordination Compounds, "An electrochemical synthesis route to form heterojunction of BiVO4/ZnO nanodendrites for solar water splitting", 25-29 July 2023, Ulm, Germany.
4. H. Ali *et al.*, "Effect of annealing on luminescence and photocatalytic activity of ZnS nanocrystals under UV light irradiation," *NANOCON Conf. Proc. - Int. Conf. Nanomater.*, vol. 2021-October, pp. 261–266, 2021.

**Other research activities and academic stay abroad:**

1. *Research Internship* (04.2023-08.2023) in **Beránek Research Group in Institute of Electrochemistry at Ulm University** (Baden-Württemberg, Germany) under supervision of Prof. Dr. Radim Beránek. The objective of this internship is to develop a stable and low-cost nanomaterial for a use in photoelectochemical energy conversion systems.
2. *Research Internship* (09.2022-10.2022) in **Centre for Functional and Surface Functionalized Glass** (FunGlass, Trenčín, Slovakia) under supervision of Assoc. Prof. José Joaquín Velázquez García. The main motive of this mobility was to characterize thin film samples with the state-of-the-art techniques.
3. *Erasmus mobility* (09.2016-01.2017) in **Centre of Polymer Systems at Tomas Bata University** under guidance of Prof. Ivo Kuritka for master`s degree dissertation.

Ali Can Güler, M.Sc., Ph.D.

# Hybrid nanomaterials for photoanodes in photoelectrochemical water splitting

Hybridní nanomateriály pro fotoanody
k fotoelektrochemickému štěpení vody

Doctoral Thesis Summary